NONLINEAR DYNAMICS OF A NEW CELLULAR AUTOMATA MODEL

Christoforos E. Somarakis,* George P. Papavassilopoulos,† and Firdaus E. Udwadia‡
School of Electrical and Computer Engineering,
National Technical University of Athens,
GR & Department of Aerospace and Mechanincal Engineering,
University of Southern California, USA
(Dated: November 14, 2008)

In this paper a new rule in cellular automata is introduced. Through extensive simulations, visual inspection and numerical explorations, its generic dynamical behavior is outlined and classified into categories. Properties such as regular and complex behavior are reported and studied in connection with the system's parameters as well as the initial configurations and topology of the automaton state space. Further research on the rule is recommended since under certain variations (many of them are reported) this rule can be a reliable model for simulating procedures among various scientific fields.

I. INTRODUCTION AND HISTORICAL NOTES

Cellular automata are perhaps the simplest mathematical representations of complex dynamical systems. They are a class of spatially and temporally discrete, deterministic models characterized by local interaction and an inherently parallel form of evolution.
The history of cellular automata can be traced back to 1948, when *J. L. von Neumann* introduced them to study simple biological systems [8]. As his work progressed, *Neumann* started to cooperate with *S. M. Ulam*, who introduced him to the concept of cellular spaces [19]. These described the physical structure of a cellular automaton, i.e., a grid of cells which can be either "on" or "off". Shortly after, *A. M. Turing* proposed, in 1952, a model that illustrated reaction-diffusion in the context of morphogenesis [14]. In the 1970s, cellular automata found their way to one of the most popular applications called *simulation games*, of which *J. H. Conway's*, *Game of Life* is probably the most famous [3]. However, the widespread popularisation of these systems was achieved in the 1980s through the work of *S. Wolfram*. Based on empirical experiments using computers, he gave an extensive classification of cellular automata as mathematical models for self-organising statistical systems (collected papers in [19]). *Wolfram's* systematic research is to relate cellular automata to all disciplines of science (e.g., sociology, biology, physics, mathematics, economy, *etc*).
In this paper, we will introduce a new model (we shall call it the $\mathcal{F}$-*rule*). This model came as a result of comprehensive research in dynamical structures of networks as these were constructed out of game theory and statistical physics. The $\mathcal{F}$-rule is an outgrowth of the *Prisoner's Dilemma* game as it is stated by *Nowak et all* [9]. An in-depth numerical investigation of this model was first done in [16]. In that work a slightly different version of the rule is studied where it is mainly viewed from the point of Game Theory. In this paper, we restate the model as a cellular automaton and attempt to gain a deeper understanding of its dynamics. Some preliminary results of this research are presented in [2]. This paper is a major extenstion of [2]. Here we explore our rule using various lattice dimensions and initial conditions, while all possible parameter configurations are considered. The model is primarily assumed as a dynamical system evolving in a discreet state space and time. Our aim is to classify the rule's behavior and characterize both qualitatively and quantitatively the degree of it's complexity. Varying on different state parameters and specifications drastically different behaviors are observed.

A. Notations and Definitions

Before we introduce our model, it is necessary to present some generic characteristics of cellular automata. These concepts will assist in getting a picture of the rule's dynamic behavior locally and globally.

1. The State Space

We define an Euclidean space $\mathcal{L} : \mathbb{N}^d$, where $\mathbb{N}$ is the set of natural numbers, as the discrete state space. This is the lattice of d-dimensional sites upon which our automata live, and their dynamics unfold. Every individual site can be defined by a $(1 \times d)$ vector $\overrightarrow{x}$. In our work, both one and two-dimensional state spaces are explored .

*Electronic address: cslakonas@yahoo.gr; PhD Student, E.C.E. N.T.U.A.
†Electronic address: yorgos@netmode.ntua.gr; Prof., E.C.E. N.T.U.A.
‡Electronic address: fudwadia@usc.edu; Prof., V.S.E., U.S.C.

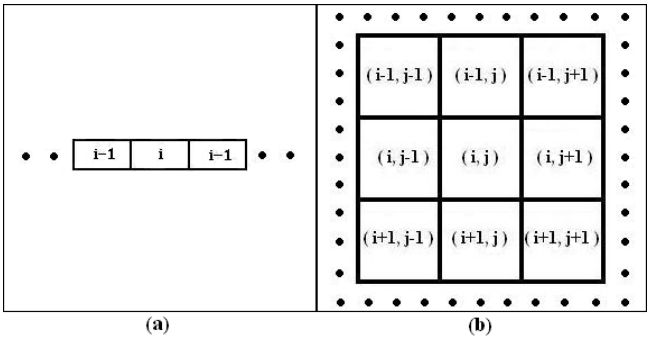

FIG. 1: The $r = 1$ neighborhood of the state spaces, outlined with the rectangular sketches. (a)The 1-D space. Each individual site i interacts with the contigious $i-1$ and $i+1$ around it. (b)The 2-D space. Every site is defined to interact with each of it's eight neighbors (the Moore's scheme).

2. Neighbourhood of a cell

Let us now define the regime of local interaction. Every cell changes it's state after communicating with it's neighboring cells. We note by $\mathcal{N}(\overrightarrow{x}, r)$ the range-r neighbourhood of $\overrightarrow{x}$,without $\overrightarrow{x}$ itself, and by $\underline{\mathcal{N}}(\overrightarrow{x}, r)$ the range-r neighborhood, including $\overrightarrow{x}$, i.e.

$$\mathcal{N}(\overrightarrow{x}, r) = \{\overrightarrow{y} \epsilon \mathcal{L} : 0 < ||\overrightarrow{x} - \overrightarrow{y}||_\infty < r\} \quad (1)$$

$$\underline{\mathcal{N}}(\overrightarrow{x}, r) = \{\overrightarrow{y} \epsilon \mathcal{L} : 0 \leq ||\overrightarrow{x} - \overrightarrow{y}||_\infty < r\} \quad (2)$$

where $||*||_\infty : \mathbb{N}^d \to \mathbb{N}$ is the infinity norm. In our work, unless otherwise stated, we suppose $r = 1$ which means that the neighbourhood of a given center site $\overrightarrow{x}$, is the set of sites which are immediately adjacent to $\overrightarrow{x}$ (see Fig.1). In 1-D dynamics this is the most common interaction scheme. On the plane this is, generally, known as *Moore's scheme* [20].

3. Local Value Space

Each cell $\overrightarrow{x} \epsilon \mathcal{L}$ can assume only a finite number of different values:

$$\sigma(\overrightarrow{x}; t) \epsilon \Sigma = \{0, 1, 2, ..., k-1\} \times \mathbb{N} \quad (3)$$

where $\sigma(\overrightarrow{x}; t)$ is the value of $\overrightarrow{x}$ at time $t \epsilon \mathbb{N}$. In our paper, we set $k = 2$. The set of possible states at time t can be either $\sigma = 0$ or $\sigma = 1$. In the following, a black-coloured site means a site in 0 state, whereas a white-coloured site is in state 1.

4. Boundary Conditions

Although cellular automata theoretically live on infinitely large lattices, computer simulations run on finite sets. Thus, it is also essential to define conditions on the boundaries of the lattices. Among various types of boundary conditions that have been proposed [19], [4] , in this paper, finite lattices are exclusively considered with *periodic* boundary conditions in both one and two dimensions.

5. Initial Conditions

In the following, we will implement our model in two types of lattices. In the one-dimensional and in the two-dimensional space. In each of these sections there will be two sorts of initial configurations.
The *simple seeds*. Here the system starts from a pattern full of cells at state 1 (white) except one single cell that is in state 0 (black). The growth of cellular automata from such setup should provide models for a variety of physical and other phenomena,such as symmetric growths like crystal or snow-flake growth [19],[10].
The *random seeds*. Here, the system starts from a disordered configuration where each cell is at state 1 or 0 with equal probability $p = 1/2$. This setup reflects the notion of arbitraty initial conditions as it is known in the dynamical system theory and helps us observe the model's self-organization properties as well as the global behavior of cells under certain parameter values.

B. The $\mathcal{F}$-Rule

Having specified our cellular world, we now move on to define the transition rule under which every site $\mathcal{L}$ is updated. To each $\overrightarrow{x} \epsilon \mathcal{L}$, we assign a cost function $V(\overrightarrow{x}, \mathcal{N}(\overrightarrow{x}); t) : \Sigma^2 \times \mathbb{N} \to W = \{a, b, c, d\} \subset \mathbb{R}$ such that:

$$V(\overrightarrow{x}, \overrightarrow{y}; t) = \begin{cases} a & \text{if } \sigma(\overrightarrow{x}; t) = \sigma(\overrightarrow{y}; t) = 0 \\ b & \text{if } \sigma(\overrightarrow{x}; t) = 0, \sigma(\overrightarrow{y}; t) = 1 \\ c & \text{if } \sigma(\overrightarrow{x}; t) = 1, \sigma(\overrightarrow{y}; t) = 0 \\ d & \text{if } \sigma(\overrightarrow{x}; t) = \sigma(\overrightarrow{y}; t) = 1 \end{cases} \quad (4)$$

These costs reflect the tension of local interactions between individual cells. So, the initial step of our rule is that for a fixed value $\sigma(\overrightarrow{x}; t)$ and for every $\sigma(\overrightarrow{y}; t)$ of $\overrightarrow{y} \epsilon \mathcal{N}(\overrightarrow{x})$ we adjust a number $w \epsilon W$ to $\overrightarrow{x}$. Finally, for a fixed arrangement of states in $\mathcal{N}(\overrightarrow{x})$, site $\overrightarrow{x}$ receives an overall cost:

$$\mathcal{V}(\overrightarrow{x}; t) = \sum_{\overrightarrow{y} \epsilon \mathcal{N}(\overrightarrow{x})} V(\overrightarrow{x}, \overrightarrow{y}; t) \quad (5)$$

Or in the analytic form:

$$\mathcal{V}(\overrightarrow{x}; t) = (1 - \sigma(\overrightarrow{x}; t)) \left\{ \sum_{\overrightarrow{y} \epsilon \mathcal{N}(\overrightarrow{x})} \Big[a(1 - \sigma(\overrightarrow{y}; t)) + b\sigma(\overrightarrow{y}; t) \Big] \right\} + \\ + \sigma(\overrightarrow{x}; t) \left\{ \sum_{\overrightarrow{y} \epsilon \mathcal{N}(\overrightarrow{x})} \Big[c(1 - \sigma(\overrightarrow{y}; t)) + d\sigma(\overrightarrow{y}; t) \Big] \right\} \quad (6)$$

Finally, $\forall \overrightarrow{x} \epsilon \mathcal{L}$, $\overrightarrow{z} \epsilon \underline{\mathcal{N}}(\overrightarrow{x})$ the update rule is defined to be:

$$\sigma(\overrightarrow{x}; t+1) = \mathcal{F}(\sigma(\overrightarrow{z}; t)) = \sigma(\overrightarrow{z}; t)$$
$$\text{s.t. } \left\{ \overrightarrow{z} \epsilon \underline{\mathcal{N}}(\overrightarrow{x}),\ \mathcal{V}(\overrightarrow{z}; t) = \max_{\overrightarrow{z} \epsilon \underline{\mathcal{N}}(\overrightarrow{x})} \left\{ \mathcal{V}(\overrightarrow{z}; t) \right\} \right\} \quad (7)$$

In case there are more than one neighbors with same maximum $\mathcal{V}$ but in different state we avoid the conflict by setting $\overrightarrow{x}$ to follow the white neighbor. We denote by $\mathcal{F}_{(a,b,c,d)}$ the $\mathcal{F} - rule$ with the specific cost parameters.

1. Properties and Remarks

It can be easily shown that:

$$1.\ \mathcal{F}_{(a,b,c,d)} \equiv \mathcal{F}_{(a+q,b+q,c+q,d+q)} \quad \forall\ q\ \epsilon\ \mathbb{R} \quad (8a)$$
$$2.\ \mathcal{F}_{(a,b,c,d)} \equiv \mathcal{F}_{(aq,bq,cq,dq)} \quad \forall\ q\ \epsilon\ \mathbb{R}_+ \quad (8b)$$
$$3.\ \mathcal{F}_{(a,b,c,d)} \equiv \mathcal{L}_1 \oplus_2 \mathcal{F}_{(d,c,b,a)} \quad (8c)$$

The first two properties signify the model's invariance under additivity and multiplication, while the third property states that the inverse of the opposite-cost rule equals the straight-forward one.

At this point, we will make some remarks concerning the nature of this model. First, the $\mathcal{F}$-rule is a *purely deterministic dynamic procedure*. Neither stochastic fluctuations, nor any sort of noise, affect the evolution of the cells. Second, one may easily notice that the a and d costs reflect the local interaction among cells in the same state. Similarly, the b and c costs reflect the local interaction among cells with opposite states. In the following, we shall refer to a, d as *equal-state* and to b, c as *cross-state* costs. Moreover, a carefull insight into the rule's local behavior reveals that the interactions are in fact within a range $r = 2$ rather than $r = 1$. In the previous paragragh we noted that the decision of $\sigma(\overrightarrow{x}; t+1)$ depends on the values of $\mathcal{V}(\overrightarrow{z}\ \epsilon\ \underline{\mathcal{N}}(\overrightarrow{x}); t)$. However, every cost $\mathcal{V}$ is, subsequently, a result of local interaction between the neighbours of the center site and their own neighbors. What, actually, happens is the local alternation of two, interconnected, procedures. On our N^d $(d = 1, 2)$ lattice $\mathcal{L}$ of $\sigma = 0, 1$ states, the power set of $\mathcal{L}$: is noted as $\mathcal{P}(N^d)$, and consists of 2^{N^d} elements which take values from Σ. In other words $\mathcal{P}(N^d)$ is the set of all possible states of the pattern. We also denote by $J(t)$ the state of cost values of $\mathcal{L}$ at time t. Now if $G(t)\ \epsilon\ \mathcal{P}(N^d)$ is the global state of the system at time t then $\mathcal{F}$-rule can be separated into alternating between two sub-rules:

$$\mathcal{F} = \begin{cases} f_1 : G(t) \to J(t) \\ f_2 : J(t) \to G(t+1) \end{cases} \quad (9)$$

where f_1 is the function that sets the costs out of the states and f_2 is the function that updates the (new) states out of the costs. In this work we will generally investigate the behavior of lattice states G. It would be very interesting, though, to study the states of costs J and interpret them in conjuction with the G set.

Hoping that, by this point, our model is understood, our next questions arise intuitively."What is so interesting about this rule?", "What kind of behavior is this rule capable of exhibiting?". We will provide some answers by running simulations. As we have mentioned in [2], an analytical approach of the solution of the model is extremely difficult. For this reason we simulated the rule, examining every possible combination of the payoff parameters a, b, c and d. In the simple seed initial conditions we will work as follows: We will, first, assume $a < d$. Then $(8a)$ implies that we can only consider positive values of the parameteres. Additionally, from $(8b)$ we can set $a = 0$ and $d = 1$ and with no loss of generality let $b,\ c$ free. Similarly, we will, then, consider the case $a > d$ $(a = 1,\ d = 0)$. Varying the cross-interaction parameters we will see how differently the system behaves and how, for some critical values, the system alters from "regular" to "irregular" behavior. Moreover, in the 2-D case, we will see that the system's behavior also changes by varying the lattice's topology. In the random setups we will work in a similar manner.

II. THE 1-D $\mathcal{F}$-RULE

Our exporation of the model begins by implementing it in an one-dimensional strip (Fig. 1(a)) and projecting it's evolution. The dynamics in this case are rather simple as one can see in Fig. 2. Varying the b, c cost parameters, four types of evolution are, all in all, observed.

In case of $a = 0, d = 1$ the occuring parameterization is:

(a) $c \geq 2b - 1$ The system evolves to homogeneous state. All sites get to $\sigma = 1$ (Fig. 2(a)).

(b) $1/2 < b \leq 1, c < 2b - 1$ In simple seeds the system, directly, stays static for all time (Fig. 2(b)).

(c) $1 < b \leq 2, c < b - 1$ The system expands at the first step and reaches a static equilibrium (Fig. 2(c)).

(d) $b > 1, c \geq b - 1$ The system, directly, evolves to period 2 oscillation (Fig. 2(d)).

(e) $b > 2, c < b - 1$ The system converges to homogeneous state. All sites, eventually, get to $\sigma = 0$ (Fig. 2(e)).

In case of $a = 1, d = 0$, we have:

(a) $c \geq 2b$ The system, directly, evolves to a uniform state (Fig. 2(a))

(b) $b > 1, b + 1 \leq c < 2b$ In simple seeds the system directly evolves to period 2 where in random seed it may converge to period 2 behavior. (Fig. 2(c))

(c) $c < \min\{2, 2b, 1 + b\}$ The system converges to homogeneous black global state.(Fig. 2(e))

Using Wolfram's notification [18], $\mathcal{F}$ in one dimension generates patterns of class $c1$ and $c2$ only. Namely, the patterns that evolve after a finite number of steps to a unique homogeneous state, in which all sites have the same value. We see such behavior in Figs. 2(a),(e). These rules may be considered to evolve to simple limit points in phase space; their evolution completely destroys any information on the initial state. The spatial and temporal dimensions for such attractors are zero. In class $c2$, we have simple stable states of periodic structures (Figs. 2(b)-(d)). The dynamics become far more complex in the 2-D case.

III. THE 2-D $\mathcal{F}$-RULE

A. Evolution from Simple Seeds

Given the initial setup, the evolution of our automaton depends on the relative values of the b and c parameters as they were set by the $\mathcal{V}$-costs. We continue from [2] to further examine the effect of these payoff values. In that premilinary paper we took a few analytical steps in order to sketch the mechanism of the rule as a function of the payoffs. Case $a < d$ was only examined and led to a phase-transition diagram among regular and irregular patterns. Here, together with this plot, we also examine the case $a > d$. For the simple-seed setup, nine different schemes have been identified (Figs. 4 and 5):

P0 : The system *directly* (i.e. without transient states) evolves to homogeneous state where all cells attain the same value (i.e. $\sigma = 1$).

PT0 : The system, after a transient behavior, evolves to the homogeneous state $\sigma = 1$

P1 : The system directly evolves to periodic behavior of period 1.

PT1 : The system expands in the first iteration and remains static ever after.

P2 : The system directly evolves to periodic behavior of period 2.

P3 : The system directly evolves to periodic behavior of period 3.

PT4 : The system, after a transient behavior, evolves to period 4.

C : The system exhibits an irregular complex behavior.

B : The systems grows uniformly. At each time step, a regular patter with a fixed density of zero sites is produced.

In Fig 3(a), we present a raw phase transition pattern on the (b, c) plane for $a < d$ and in Fig 3(b) a window of the region denoted by **C** (see below for more). The phase-transition diagram when $a > d$ is sketched in Fig. 4. Moving along the diagrams' boundary lines we deal with the set of critical (bifurcation) values. For instance, in Fig 3(a) at the **PT1**, **C** boundary we step on the critical vertical line of $b = 8/5$. Similarly, the **C** to **B** boundary consists of the connected lines $b = 8/3$ and $c = b - 5/3$ [2]. For the moment we are, primarily, interested in investigating this "irregular" **C** region.

B. The C region

Contrary to the other sections, **C** is a parameter subspace, where the automaton appears to exhibit extraordinary dynamical behavior. The $\mathcal{F}$-rule in this region generates exclusively expanding patterns. In Fig. 6 we put a few of these carpets where snapshots of their evolution is presented. Every subfigure contains the plane pattern as well as a space time evolution of the lattice's main diagonal line (the line that includes the initial black cell). Unlike the other regions, these carpets have no simple faceted form and in most cases non-uniform interior. Additionally, due to symmetric initial states, these patterns are completely invariant under all the rotation and reflection symmetry transformations. In order to identify part of the **C** dynamics, we implemented various techniques presented below. Our first step was to numerically estimate the transition phase space for the individual cases $a < d$ and $a > d$. Part of these diagrams are presented in Fig 3(b). One may notice that **C** is a collection of mutually disjoint subsets of (b, c)-plane. Moreover, these subsets have occurred out of subsequent straight line intersections. In every of these subsets, our system generates the same pattern and, of course, exhibits the same dynamic behavior. So the following question would be "what is this dynamic evolution?" We will respond to this question by presenting numerical results coming out of different simulation techniques.

1. *Global dynamics on a finite, fixed $\mathcal{L}$*

At first we kept the lattice size constant (at $N = 50$) with periodic boundary conditions and we explored the system's long term behavior. Each simulation test was run for at most $20,000$ iterations. The dynamic behavior is, classified in three qualitative categories:

$\mathcal{C}_1$ After a transient behavior, all sites of $\mathcal{L}$, eventually, attain the same value. A class similar to **PT0** type (see Fig) but with much longer and more complicated transient time. Here the patterns begin to expand until their frontiers meet. Then, the overall automaton appears like a collection of travelling waves that interact with each other until they totally fade out.

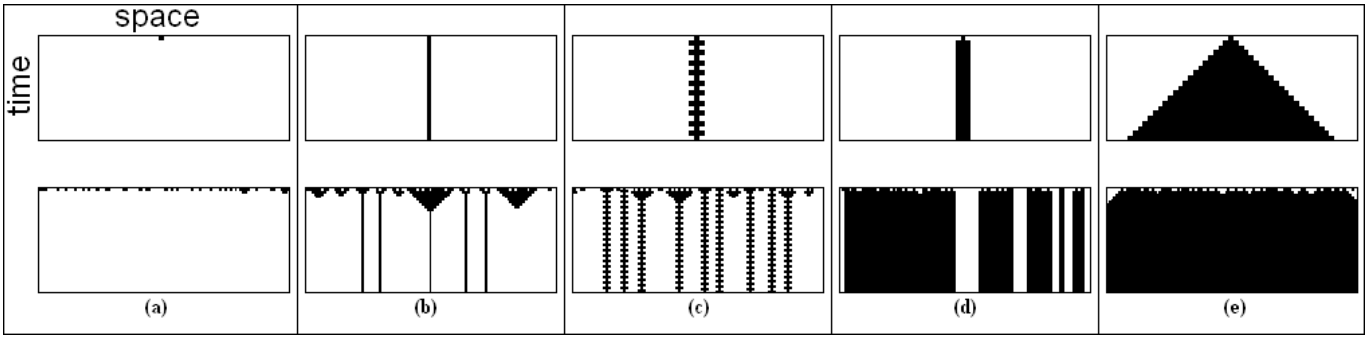

FIG. 2: The 1-D $\mathcal{F}$-rule and the patterns that are generated. The dynamics in one dimension are smooth and regular.

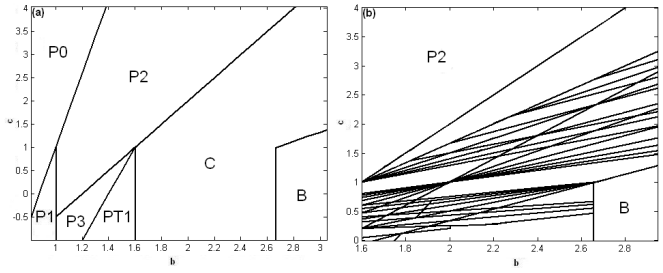

FIG. 3: The case $a = 0, d = 1$.(a)A parameter window of the (b, c)-plane, were we have sketched a rough phase transition. While regions **P0**,**P1**,**PT1**,**P2**,**P3** and **B** show regular dynamics, region **C** is rich in irregular behavior. (b)The phase transition focused on the **C** region ($1.6 < b < 2.9$). See text for explanation. The linear boundaries were numerically estimated. The calculation's precision is 10^{-3}.

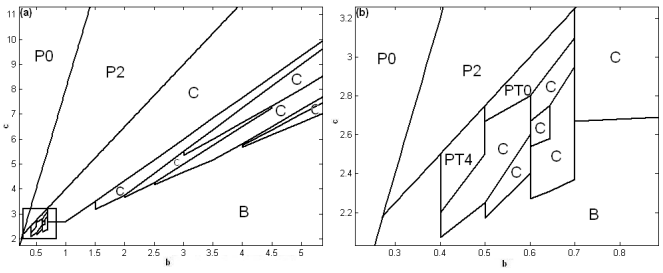

FIG. 4: The case $a = 1, d = 0$. (a)A window of the $(b - c)$ parameter subspace as it is numerically calculated. (b) Here a magnification of the rectangular area of Fig. 4(a). All regions have been assigned to a symbol characterising the generated patterns. See text for more.

$\mathcal{C}_2$ After a transient behavior, all sites of $\mathcal{L}$, converge to strictly periodic (period-T) motion. By *strictly periodic of period T* we mean that $\exists\, t \,\epsilon\, \mathbb{N} :\ \sigma(\overrightarrow{x}; t) = \sigma(\overrightarrow{x}; t + T)\ \forall\ \overrightarrow{x}\ \epsilon\ \mathcal{L}$. The difference from $\mathcal{C}_1$ is, obvisously, in the system's final state. Here our model exhibits periodic oscillations. It is observed that both the transient and the period time are quantities highly dependent on the neighborhood definition and the lattice topology. In the following paragraph, we will present an alternative type of periodic structure as a result of varying the magnitude of the lattice.

$\mathcal{C}_3$ The dynamic evolution does not converge to any of the previous two classes. A typical class $\mathcal{C}_3$ behavior is the one that after a sufficiently large number of iterations (approx. $(20,000)$) the pattern neither, strictly, repeats itself, nor turns out to a homogeneous state.

For case $a < d$ detailed numerical results concerning the transient time and the steady-state period can be found in [2].

2. *Global dynamics on a finite, varied $\mathcal{L}$*

A different approach is to explore the system's behavior by varying, instead of the (b, c) parameters, the lattice's structure. In this section, our control parameter will be size, N. We will show that many of the above analysis and classifying results are in fact dependent on the size of lattice. A simple but fundamendal statistical tool that we will use, is the average fraction of sites at $\sigma(\overrightarrow{x}; t) = 1$:

$$\rho(t) = \frac{\#_1(t)}{\#_0(t) + \#_1(t)} = \frac{\#_1(t)}{N^2} \qquad (10)$$

where by $\#_\sigma(t)$ we denote the number of cells' at time t and state σ. We will work with two characteristic models:

- $\mathcal{F}_{(0,1.65,0,1)}$. On a 50×50 matrix this is a class $\mathcal{C}_1$ rule [2]. Is this true for all N, though? In Fig. 7(a) we see the results of the system's *converging behavior*. The x-axis is the size N of the lattice $(N \times N)$ and the y-axis is the number of iterations the rule takes to turn to a global zero (black) state. For $N = 30$ all cells will be black after $t = 29$ iterations. For $N = 40$ the same holds for $t = 184$ while for $N = 50$, $t = 101$. Finally for $N = 70$ our rule needs 2510 steps to converge. However, when $N = 74$ the system does not converge to black. Instead, after thousands of iterations it returns to a

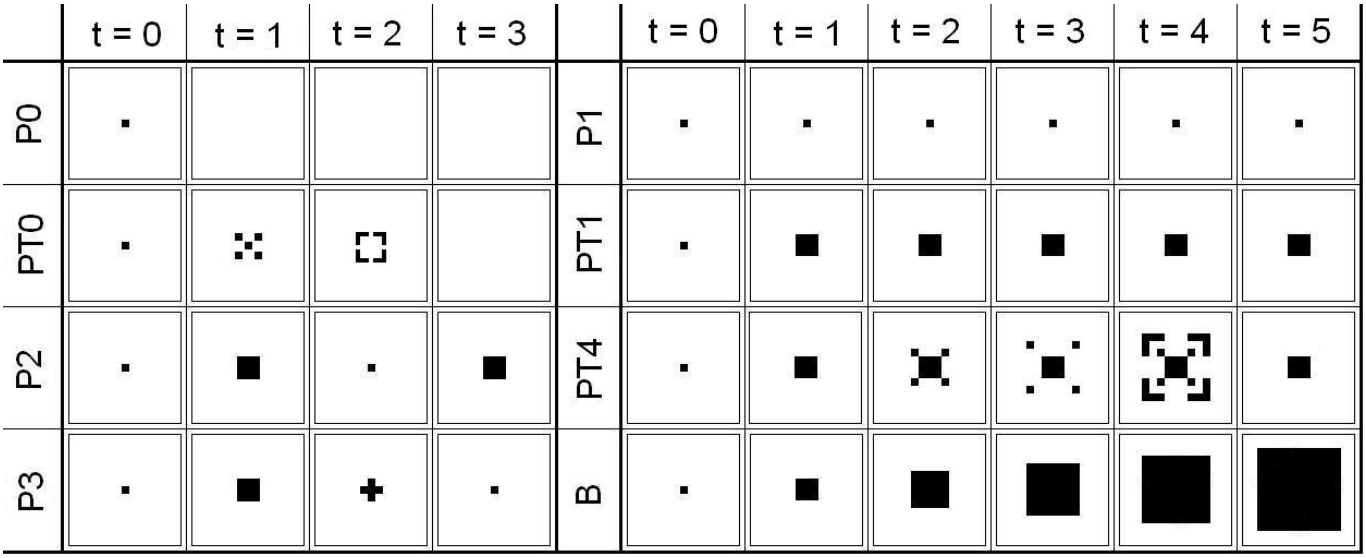

FIG. 5: Typical patterns of regular behavior of the $\mathcal{F}$-rule. When $a < d$, **P0**, **P1**, **PT1**, **P2**, **P3** and **B** appear, while in $a > d$ **P0**, **PT0**, **P2**, **PT4** and **B** appear. See text for more.

previous state but not in the strict sense, we defined above. In Fig. 8(a) we present this new type of behavior. The state of the system at $t = 4983$ becomes the same as it's state at $t = 85$, under the obvious smooth transformation of the axes. This is a new type of periodic behavior not observed until now. One may argue that since the cellular automaton will anyway turn to strictly periodicity, the behavior in question is just a trivial transient phenomenon. This is not the point, however. Our point here is that not only the dynamic classification presented above depends on the lattice's topology; but also that if we trace the time subsequence $(85, 4983, 9881, 14779, ...)$ we observe a coordinates' transformation: The system transposes by $N/2$ units up and rotates by 90^o counterclockwise. This trivial type of transformation may, however, not be the canon. During a dynamic evolution, it is highly possible that more interesting subsequences (i.e. arbitrary units and degrees shifts) exist, such that the system propagates along the donut-like $\mathcal{L}$ structurally invariant.

- $\mathcal{F}_{(1,0.6,2.67,0)}$. This pattern, presented in Fig. 6(d), is generated by a highly unstable rule the dynamics of which are presented in Fig. 7(b). The square-edged curve shows the time the rule takes to converge to periodic attractors. The circle-edged curve shows the attractor's period as a function of size N. We see, for example, that on a 10×10 $\mathcal{L}$ the rule converges to global white state, 10 iterations later (class $\mathcal{C}_1$). On a 40×40 lattice it converges to period-24 oscillation after 4 iterations, while for $N = 50$, after 33 transient steps, it settles down to a period-56 circle (class $\mathcal{C}_2$). The periodic behavior disappears for $N \geq 90$ where the system seizes to converge (class $\mathcal{C}_3$).

C. Complex Behavior

In this section, we will provide sufficient evidence to argue that the $\mathcal{F}$-rule is rightfully characterized as complex. The cost parameters belong to **C** classes. The system initiates from a simple-seed configuration and evolves on a large size (practically infinite) matrix $\mathcal{L}$.

1. *Growth Dimensions*

The limiting structure of patterns generated by the growth of cellular automata from simple seeds can be characterized by various *growth dimensions*. The type of dimension we will make use of depends on the *boundary* of the pattern. The boundary may be defined as the set of sites that can be reached by some path on the lattice that begins at infinity and does not cross any nonzero sites. This set of limiting cells can thus be found by a simple recursive procedure:

$$D_g = \lim_{t\to\infty} \frac{log(\#_0(t))}{\log(t)} \tag{11}$$

Where $\#_0(t)$ is the number of black cells generated at time t, already defined in (9). Growth dimensions, in general, describe the logarithmic asymptotic scaling of the total sizes of patterns with their linear dimensions.One may define upper and lower spatial growth dimensions D_g^+, D_g^- in terms of the upper and lower limits, lim sup

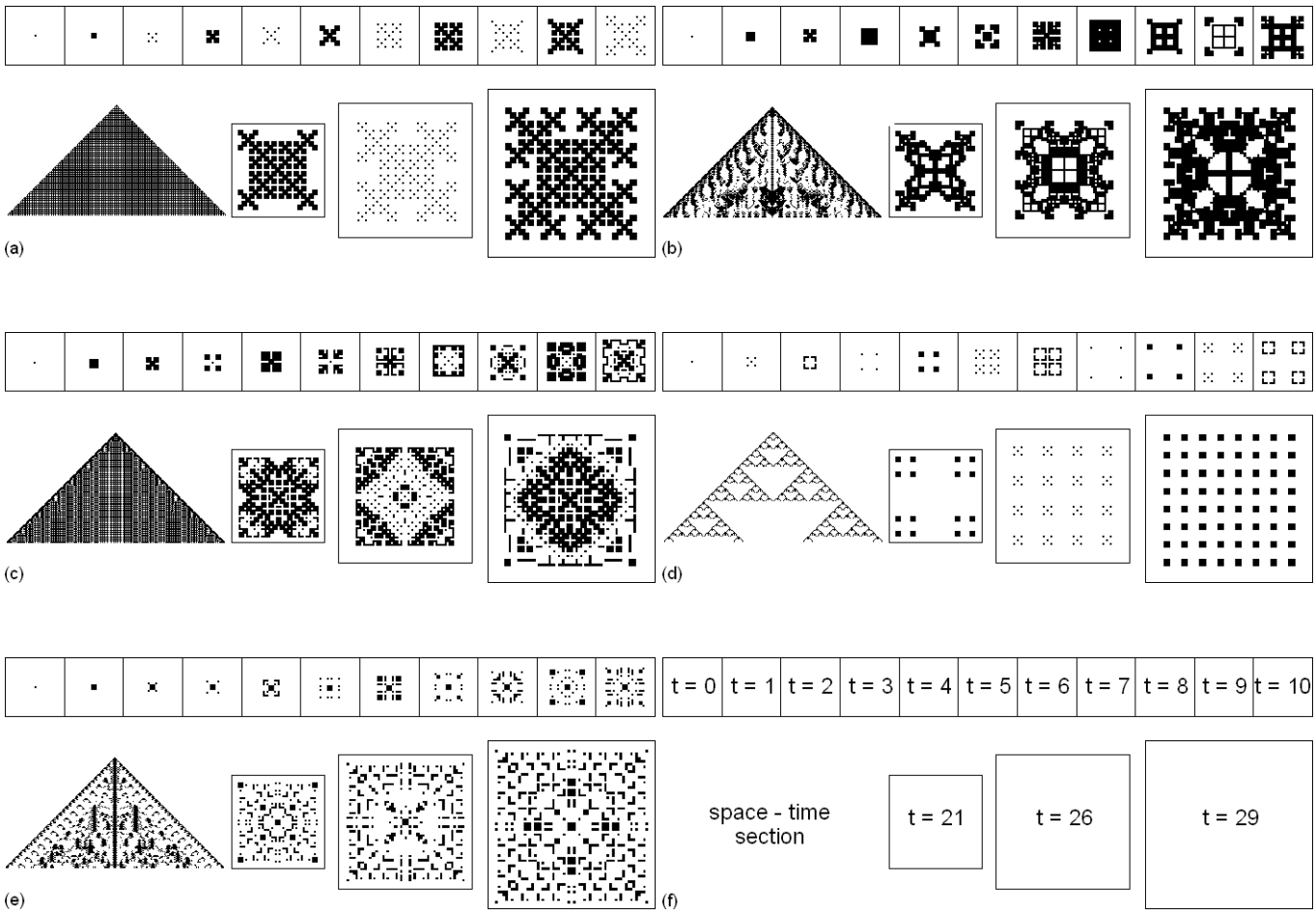

FIG. 6: Typical **C**-type patterns. (a)$\mathcal{F}_{(0,1.65,1.0834,1)}$, (b)$\mathcal{F}_{(0,1.65,0.2375,1)}$, (c)$\mathcal{F}_{(0,2.6,2.52,1)}$, (d)$\mathcal{F}_{(1,0.6,2.67,0)}$, (e)$\mathcal{F}_{(1,0.6,2.4,0)}$, (f) Explanatory map of the evolving dynamics. The space-time section is the temporal projection of the square lattice's main diagonal line of cells.

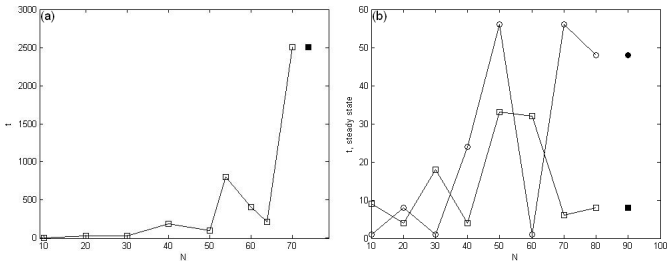

FIG. 7: (a)Code $\mathcal{F}_{(0,1.65,0,1)}$. The length of transient state of this rule as a function of lattice's size, N. For N<74 the system always converges to $\sigma(G) = 0$. For $N = 74$, however, the final state of the rule changes and a new type of periodic behavior emerges (see text). (b)Code $\mathcal{F}_{(1,0.6,2.67,0)}$. This rule passes through all dynamic classes as N varies (see text for more). The square-edged curve represents the transient time length and the circle-edge curve the steady state period.

and lim inf respectively, of $\log \#_0(t)/\log t$ at $t \to \infty$. In Fig. 9 we present $log - log$ plots of some rules: In case (a) where we have dendritic boundary growth (see Fig. 6(a)) $D_g = 1.98 \pm 0.01$. In case (b) (Fig. 6(b)) there is both non-uniform interior and boundary evolution and we have $D_g = 2.1 \pm 0.02$. In case (c) (Fig. 6(e)) the expanding pattern creates non-uniform interior while the boundaries remain faceted and $D = 1.9 \pm 0.01$. Finally, in case (d) (Fig. 6(d)) $\log \#_0(t)$ varies irregularly with $\log(t)$ the most; there $D_g^+ = 2, D_g^- = 0$. On superficial inspection of this index, class **C** patterns appear to generally satisfy these asymptotic values.

2. *Space-Time Patterns*

A direct technique of examining the asymptotical behavior of plane cellular automata is through a state subspace analysis. One may choose to define Poincaré-like sections and study the dynamic evolution of this subspace. We chose the diagonal line of the two-dimensional lattice with time (as in Fig. 6). The reason this specific section is selected is that it is the axis of sym-

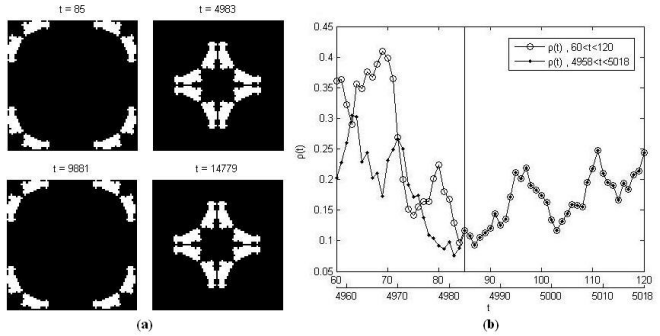

FIG. 8: Snapshots of $\mathcal{F}_{(0,1.61,0,1)}$ and N=74. We present four shots of the lattice, at $t = 85, 4983, 9881$ and 14779 respectively, where we depict this special type of periodicity. Next to those lattices, there are the ρ curves of the same orbit but at different time intervals. We can clearly see that after the vertical limit line we have set, the density of white cells is the same, proving the periodic structure.

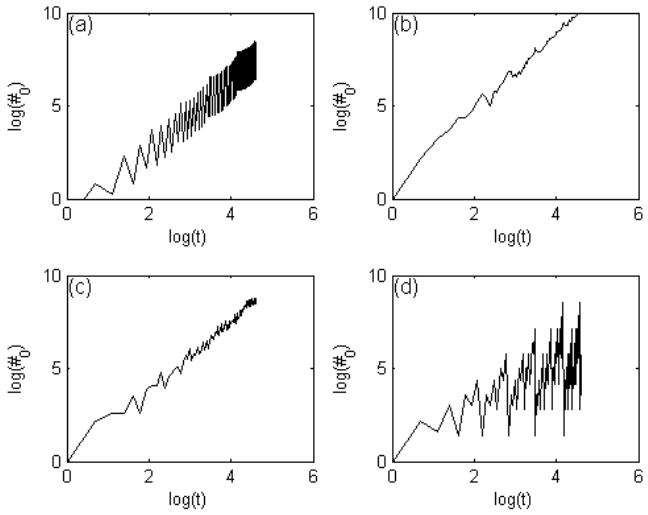

FIG. 9: Growth dimensions defined as the ratio of the logarithm of black cells over the logarithm of time. The presented codes are: (a)$\mathcal{F}_{(0,1.65,1.0834,1)}$ (b)$\mathcal{F}_{(0,1.65,0.2375,1)}$ (c)$\mathcal{F}_{(1,0.6,2.4,0)}$ (d)$\mathcal{F}_{(1,0.6,2.67,0)}$.

metry on which the system expands more rapidly than any other direction. One might also consider the main horizontal axis [2]. Moreover, we surely prefer to deal with one-dimensional patterns since such automata are, more effectively, handled. In Figs. 6(a)-(e) we present examples of space-time sections which reflect the dynamics of the 2D $\mathcal{F}$-rule in one dimension. Eq. (11) can also be applied here: (a) $D_g = 1$, (b) $D_g^+ = 0.947 \pm 0.002, D_g^- = 0.8629 \pm 0.001$ (c) $D_g = 0.99 \pm 0.01$ (d) $D_g = 1.161 \pm 0.003$ (it is noted here that the space-time section is the *Sierpinski gasket*, a self-similar object with $D_{fractal} = \log 3/\log 2 \backsimeq 1.58$).

IV. EVOLUTION FROM RANDOM SEEDS

A (completely) random seed configuration results when each site $\overrightarrow{x} \epsilon \mathcal{L}$ chooses to be black or white with probability ($p = 1/2$). Such disordered configurations are members of the set of all possible configurations. Patterns generated from them are thus typical of those obtained with any initial state. The presence of structure in these patterns is an indication of self-organization on the lattice [20]. Qualitatively speaking, three types of collective global behavior have been identified.

A. Equal-State costs greater than Cross-State costs. a,d > b,c

In this case, the evolution favors the interaction among cells with the same states. The final state of the system is a static equilibrium where the occuring pattern is an assembly of black and white "ghettos" as in Fig. 10(a). We see that the state at $t = 0$ (completely disordered). The system reaches the equilibrium within the first seven time steps. The last diagram presents index $\rho(t)$ (see figure's comments for more). Every cell on the lattice has in its neighborhood a cell of the same state and maximum cost:

$$\forall\ \overrightarrow{x}\ \epsilon\ \mathcal{L}\ \exists\ \overrightarrow{z}\ \epsilon\ \underline{\mathcal{N}}(\overrightarrow{x}, 1) : \sigma(\overrightarrow{x}) = \sigma(\overrightarrow{z})$$
$$where\ \ \mathcal{V}(\overrightarrow{z}) = \max_{\overrightarrow{z}\epsilon\underline{\mathcal{N}}(\overrightarrow{x})} \mathcal{V}(\overrightarrow{z}) \tag{12}$$

If we increase one of the two leading parameters, say a, we will observe the increase of the black sites over white. In fact, it has been analytically derived that for $a > a_c = 8/7$ all sites attain the same (black) state. The same holds, of course, if we turn d over a. The role of b, c parameters, as long as they do not exceed a and b, is that of controlling the average number of black and white cells respectively. See table I. For such non-zero values of the intermediate costs we have the critical inequality $7a + b > 8d$ instead of a_c.

B. Cross-State costs greater than Equal-State costs. b,c > a,d

Completely different patterns occur when "cross-state" costs b, c are larger than "equal-state" costs a, d. The typical code for this family is $\mathcal{F}_{(0,1,1,0)}$ a simulation of which is presented in Fig. 10(b). The system after a transient mode of 65 time steps, settles down to a period-10 cycle. One may notice the black and white regions inside of which there are white and black kernels, respectively. They are these cellular kernels that, actually, motivate this oscillation. Observe that in Fig. 10(b) the sketches at $t = 76$ and at $t = 77$ are almost inverted images. We rightfully call this behavior a *ying-yang* oscillation. In

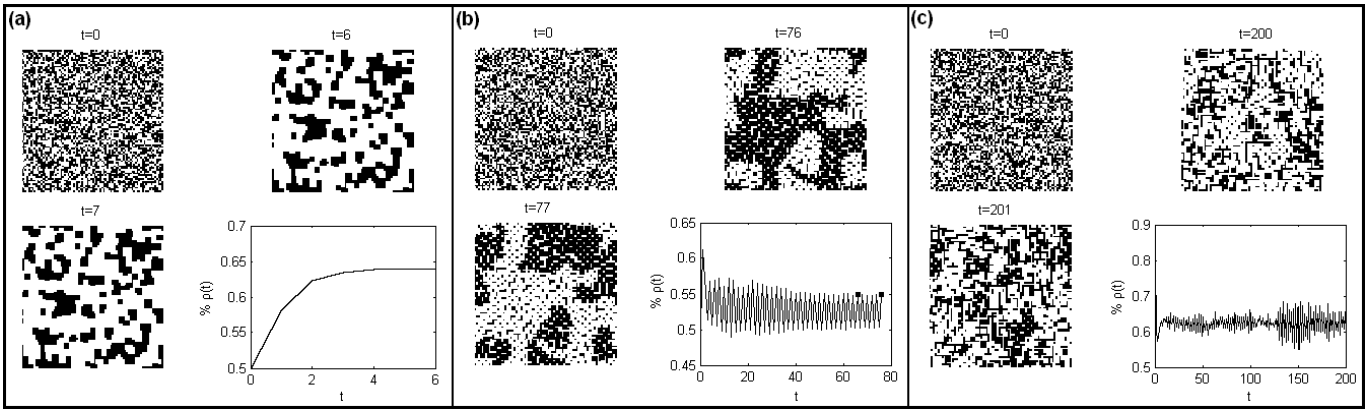

FIG. 10: The $\mathcal{F}$ model starting from random seeds. (a) $\mathcal{F}_{(1,0,0,1)}$ - the system reaches a static final state. (b)$\mathcal{F}_{(0,1,1,0)}$- the system oscillates in a period-10 cycle. (c) $\mathcal{F}_{(0.5001,0.5,1,0)}$- the system behaves aperiodically.

b	c	index $\overline{\rho}(t)$ %
0	0	63.35
0	0.1	37.57
0	0.2	37.58
0	0.3	28.72
0	0.4	22.14
0	0.5	18.08
0.1	0.2	36.50
0.3	0.2	63.25

TABLE I: The role of cross-state costs and their effect on the black and white population. Increasing b the black cells raise over white, while increasing c the white cells raise over black. This holds as long as both b and c stay lower than a and d. Otherwise, new dynamics occur.

general, an $\mathcal{F}_{(a,b,c,d)}$ where $b, c > a, d$ generates orbits that after a transient time converge to periodic attractors. The qualifying formula of this family is:

$$\forall\ \overrightarrow{x}\ \epsilon\ \mathcal{L}\ \exists\ \overrightarrow{z}\ \epsilon\ \underline{\mathcal{N}}(\overrightarrow{x}, 2) : \sigma(\overrightarrow{x}) = \sigma(\overrightarrow{z})$$
$$where\ \ \mathcal{V}(\overrightarrow{z}) = \max_{\overrightarrow{z}\,\epsilon\underline{\mathcal{N}}(\overrightarrow{x})} \mathcal{V}(\overrightarrow{z}) \tag{13}$$

The transient time, the period of the attractor and the *magnitude of oscillation* $\rho(t)/(1-\rho(t))$ are "unpredictable" quantities. Namely, they seem independent of the cost parameters. It is unknown, though, whether these quantities depend on the initial conditions and how much. What we are only sure of is that the system will converge to even-period limit sets. The role of a, d costs is, as long as they remain lower than cross-state costs, similar to the first family. They merely stabilise the mean amount of black and white cells respectively, in other words, the mean value of ρ in steady state.

C. One Equal-State parameter is between the Cross-State parameters. $d < b < a < c$

The last case is studied by fixing $d = 0, b = 0.5, c = 1$ and vary a. We then increased parameter a from $a = 0$. The moment a jumps over b a new type of behavior appears. In particular, for:

(a) $0 < a < b = 1/2$. The system behaves like in the previous case since we have $b, c > a, d$. The attractors are of even period and the mean value of $\rho(t)$ is around 0.63.

(b) $1/2 < a < 2/3$. The system does not converge. Here a typical rule is $\mathcal{F}_{(0.5001,0.5,1,0)}$ which we present in Fig. 10(c) and study ever after. Like in the case of simple seeds we have simulated the model for about $20,000$ iterations. The system neither converges to a static equilibrium nor to a periodic circle. This "aperiodic" evolution in a deterministic model like ours resembles chaos. In the following, we will further support this idea.

(c) $2/3 < a < c = 1$. The system converges to periodic attractors.

(d) $a > 1$. All sites attain the zero state.

D. Stability

An important tool to characterize the evolution of an automaton is the discrete *Green function*. Green functions measure changes in patterns generated by a given rule resulting from a small change in the initial state, and give the average probability that sites a given distance away from the small area of differing initial values will be changed after a certain number of iteration steps. We can get a glimpse of the form of these Green functions for a selected rule by plotting the *difference pattern*.

These are pattern of difference between two evolutions of the same rule starting from two different initial states. The rate of growth of these patterns is defined to be

$$\Delta(n) = \mathcal{F}^n[\sigma(G_1;0)] \oplus \mathcal{F}^n[\sigma(G_2;0)] \qquad (14)$$

This rate gives an idea of the speed with which various features in a cellular automaton evolution may propagate through the lattice. The information we are interested in is the small perturbation in the initial states. Wolfram in his pioneering work was the first to, at least heuristically, introduce this idea as a technique to effectively quantify the rate of propagation of information. The asymptotical rate is a number analogous to the *Lyapunov exponents* in the dynamical systems theory. A consistent approach to these global quantities was made [12] who defined Lyapunov exponents in one dimensional cellular automata. The multidimensional case was solved by [13] a few years later who introduced the idea of *directional Lyapunov Exponents*. In our work, we generated two almost equal random setups that differ in one site. We let them run under the same $\mathcal{F}$-rule and used (13) to see the resulting effect. We used three different rules; one of each category. The results are presented in Fig. 11. In (i) we present the difference pattern after 100 iteration. In (ii) and (iii) there are the space-time sections of the horizontal and the diagonal line of the state space. These patterns represent 4 out of 8 directional exponents [21]. Finally in (iv) and (v) we present the $\rho(t)$ index of the resulting orbits. So in Fig. 11(a) there is the simulation result of $\mathcal{F}_{(1,0,0,1)}$. The initial perturbation was directly either eliminated or stabilised to a plastic difference like in Fig 11(a). This dynamic behavior signifies of the system's expected robustness in initial perturbations. A more unstable evolution appears when the cross-state costs excell the equal-state ones. In case of $\mathcal{F}_{(1,0,0,1)}$ the initial difference expands at first but finally remains localised (Fig. 11(b),(i)). Nevertheless, the system oscillates. Both the initial patterns have converged to periodic sets, the first of period 8 (see Fig. 11(b),(iv)) and the second of period 4 (Fig. 11(b),(v)). Thus the difference pattern oscillates too. It is worth saying that it is possible for the two systems to oscillate with the same period but not with the same magnitude; a quantity characterised as unpredictable in §IV**B**. Global instability is reported for the family of §IV**C** rules. In Fig. 11(c) we present the difference patter of $\mathcal{F}_{(0.5001,0.5,1,0)}$. In this category a single site perturbation is enough to lead to two totally different orbits (see 11(c),(iv) and (v)) which, nevertheless, evolve with the same $\overline{\rho}$. From space time sections we observe the linear growing difference which implies exponential divergence (asymptotical in case of infinite lattice) of nearby configurations [4],[20], i.e. chaos.

V. THE $\mathcal{F}$-RULE VERSUS THE $\mathcal{O}$-RULE.

We have so far considered our model as a system and we have worked on it from the field the dynamical systems. One should not neglect the fact, though, that the base of the rule is derived from a typical evolutionary game; the iterated Prisoner's dilemma. The $\mathcal{F}$-rule could, naturally, be considered as a game among interacting agents which can follow the strategy of being black or white. Based on the same cost function f_1 we introduce the alternative strategy as follows: the cell updates it's state so that it optimizes it's own overall cost $\mathcal{V}$:

$$\sigma(\overrightarrow{x};t+1) = \{0,1\} : \mathcal{V}(\overrightarrow{x}) = MAX \qquad (15)$$

The alternative strategy is, actually, another update function f_2 which we shall name the $\mathcal{O}_{ptimal}$-rule. We will not use these rules as possible strategies that cells can follow, though. In this scenario, all agents play only the $\mathcal{F}$-rule apart from an individual who plays only the $\mathcal{O}$-rule. Our purpose is to study the effect of this "smart" player and how this propagates to the rest of the population. We have set this player at point $(N/2+1, N/2+1)$ and have run the simulations on a $N = 80$ square lattice and three characteristic code-rules were examined. In the presented simulation below we also count the number of white sites at time step t. This is familiar, from the theory of error-correcting codes, measure known as the *Hamming distance* [19]. This will reveal the temporal respond of the overall system towards the game of the individual. The results are presented in Fig. 12.

- $\mathcal{F}_{(1,0,0,1)}$. This family of rules leads to static equilibria. The smart player will then have to follow the state of ghettos. If it is in a white neighborhood it goes white, else it goes black. In case it is on the boundary of two neighborhoods the $\mathcal{O}$-player will go with the majority of the states around. This may have a very small effect on one or two contiguous $\mathcal{F}$-players but nothing more than that. In Fig. 12(a) we present the most probable scenario in which the smart player finds itself in a homogeneous white surrounding and synchronizes it's state to the white too.

- $\mathcal{F}_{(0,1,1,0)}$. In this case, the state of cells tends to change at every iteration so that the smart player's game can be considered as a constant perturbation. Nevertheless, as one may notice the Hamming distance plot in Fig. 12(b) it's effect propagates slowly with time, as well as it finally remains localized. In other words, the difference pattern reveals a diffusive-like growth that lasts as soon as both lattices converge to a periodic cycle.

- $\mathcal{F}_{(0.5001,0.5,1,0)}$. In this, highly unstable, zone we should expect that such perturbation reflects to the pattern globally (see Fig. 12(c). It is worth comparing the Hamming distance plots of this case and the previous. Here, $H(t)$ grows almost linearly with time until it saturates due to the finite-size lattice.

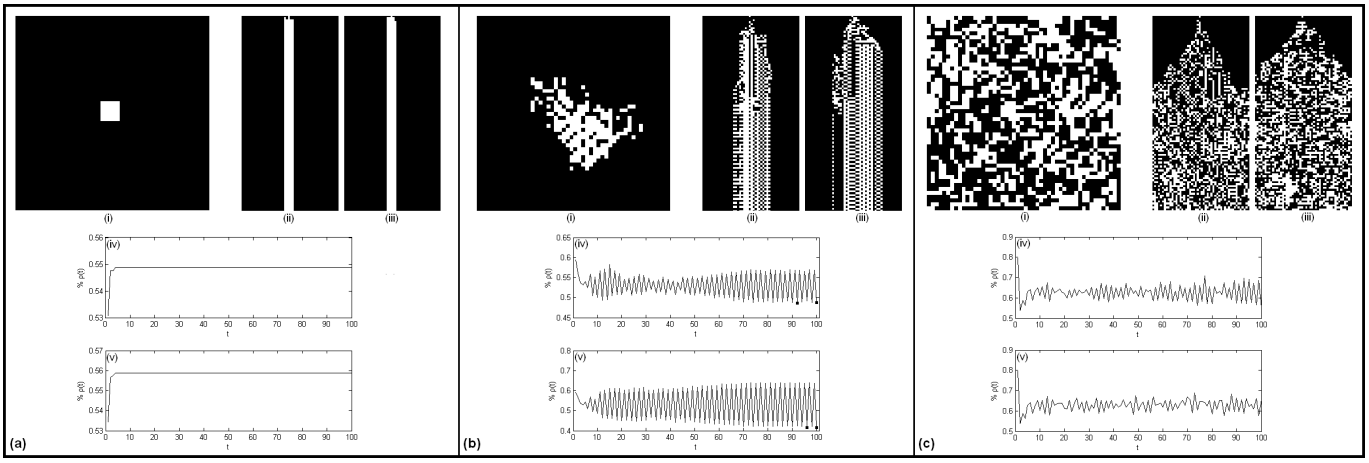

FIG. 11: Difference patterns of the $\mathcal{F}$-rule starting from random seeds.(a) $\mathcal{F}_{(1,0,0,1)}$. If there is a noticeable difference then it's range will not exceed few cells and remain plastic for all times. (b) $\mathcal{F}_{(0,1,1,0)}$. In this case the initial difference expands during the transient steps. As soon as the patterns converge to periodic attractors, the difference pattern will converge too. Hence the range of the effect is expected to be a function of transient length. In the steady-state mode, the space-time patterns produce periodic structures with the range of the resulted difference. (c) $\mathcal{F}_{(0.5001,0.5,1,0)}$. The system is highly unstable. A small disturbance is enough to cause an ever-expanding difference that eventually will propagate throughout the space. The space-time patterns produce expanding aperiodic structures. In other words, we have chaos.

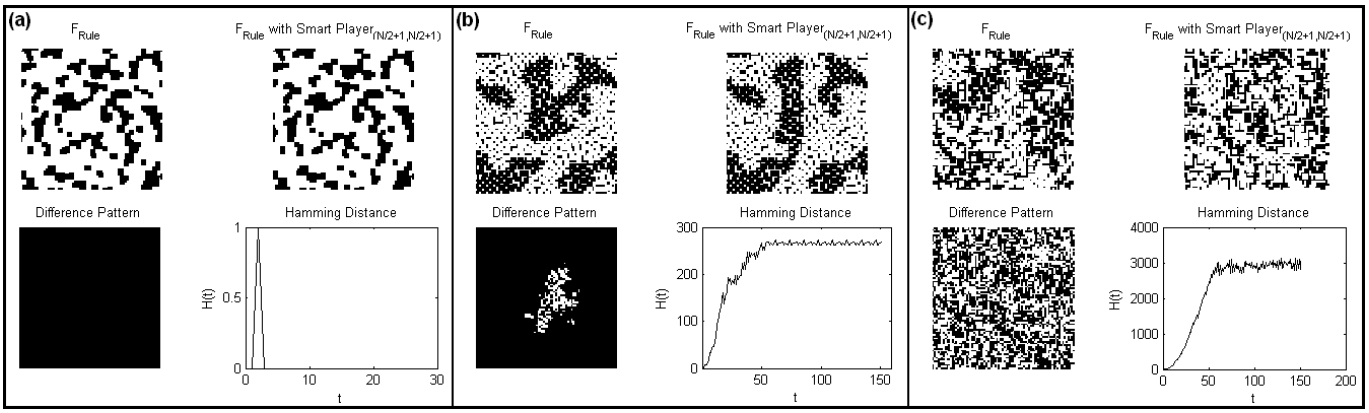

FIG. 12: $\mathcal{F}$ vs. $\mathcal{O}$. In every subfigure we present the $\mathcal{F}$-pattern, the $\mathcal{F}$ and $\mathcal{O}$-pattern, the occuring difference plot and the plot of the number of the white sites on the difference pattern versus time. (a) $\mathcal{F}_{(1,0,0,1)}$, (b) $\mathcal{F}_{(0,1,1,0)}$, (c) $\mathcal{F}_{(0.5001,0.5,1,0)}$

VI. DISCUSSION

A. Growth Inhibition

So far we have thoroughly discussed the 2-D model's transition from regular to irregular behavior. We have an idea of what happens but still do not know why this happens. The mechanism that characterizes the **C**-region is depicted in Fig.13 for the code rule $\mathcal{F}_{(0,1.65,1.0834,1)}$. At step $t = 0$ there are three costs that emerge with V_0 to be the dominating one. The automaton expands at $t = 1$ and new costs occur. Now V_2 as well as V_3 dominate their neighborhoods. However V_2 adjusts to a black cell while V_3 to a white cell. Thus, growth at $t = 1$ is allowed along the diagonals but inhibited along the horizontals and verticals. Indeed, at $t = 2$ we see the automaton has expanded at the diagonals and actually creates five black "kernels" which will at $t = 3$ expand at all directions. Iterating this procedure, the expansion will converge at an object with dendritic boundaries. This phenomenon is very common in the way some crystals grow as well as in many physical and biological systems [20],[17]. At a microspocic level the crystallization occurs when a liquid or gas is cooled below its freezing point. The procedure always start from an individual seed and unfolds by adding more frozen atoms to their surface. In some cases, whenever a piece of ice is added to the snowflake, there is some heat which is released averting the addition of further pieces in the vicinity. So, instantly, freez-

ing is allowed at some directions while it is inhibited at the rest. This effect can be simulated by a cellular automaton that updates cells to black if they have exactly one black neighbor and white if they have more than one black neighbor. This is the case in **C**-region and is clearly presented by the illustrated example. Note that at $t = 1$, V_5 has only one black neighbor while V_3 or V_4 have more than one. If growth inhibition is the base of our model's complexity on the plane, it is also the answer on the question why the 1-D $\mathcal{F}$-rule does not create irregular patterns. Using Wolfram's notification the only possible spatio-temporal patterns that can appear are of class *c1* (homogeneous black of white) or class *c2* (stable periodic). The reason of this regularity is that by definition the $\mathcal{F}$-rule, in one dimension, lacks the property of growth inhibition. A white cell in the middle of white neighbors will anyway remain white. Similarly, a black cell cannot turn to white, unless one rich white neighbor appears. This is the restricting factor of the dynamics in one dimension. It is worh noting that lifting this restriction 1-D F-rule becomes strictly chaotic. Let's define $\overline{\mathcal{F}}$ exactly as $\mathcal{F}$ but with the slight difference that when black (and only black) cell is around black neighbors it's next state will be anyway white. The resulting dynamics obey the same parameterization as in §II, but the final group of patterns is not the uniformly expanded as in Fig 2(e), but this in Fig. 14. This is a typical chaotic pattern with a self-similar strtucture.

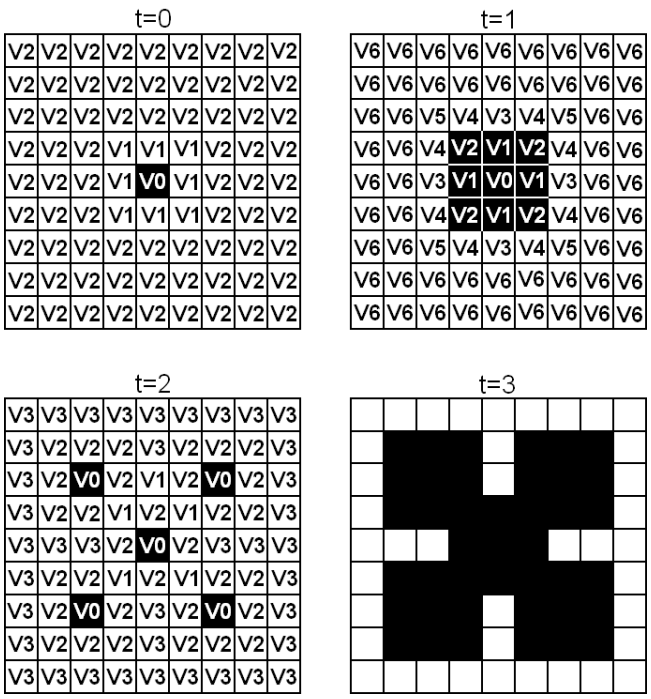

FIG. 13: Growth inhibition of $\mathcal{F}_{(0,1.65,1.0834,1)}$. At $t = 0$: $V_0 = 13.2$, $V_1 = 8.0834$, $V_2 = 8$. At $t = 1$: $V_0 = 0$, $V_1 = 4.95$, $V_2 = 8.25$, $V_3 = 8.2502$, $V_4 = 8.1668$, $V_5 = 8.0834$, $V_6 = 8$. At $t = 2$: $V_0 = 13.2$, $V_1 = 8.1668$, $V_2 = 8.0834$, $V_3 = 8$.

B. Conclusions and Remarks

The multifarious dynamic behavior of a new model is presented. We examined the model in various initial configurations, space dimensions and topologies and parameter setups. We attempted to shed light upon different aspects of the rule's dynamics and classify the collective and asymptotic behavior of the emerging patterns both qualitatively and quantitatively. The phase-transition diagramms presented in Figs. 3 and 4. We notice that in case $a < d$ the **C**-region is a significantly larger set than the one in $a > d$. This highly depends on the initial configuration that in both cases is a single black cell in a world of white cells. On the other hand, both diagramms appear as a mass of line segments while some of them are also crooked. In [2] we tried to describe the mechanism out of which all this linear boundaries emerge. We only mention here that all these bifurcation lines (as well as every critical cost value) depend on the definition of neighborhood. In this work we have adopted the Moore's scheme. Be assured that with another scheme, new phase transition properties will take place. But it is not only the local interaction regime that plays a crucial role in our work. In the dynamics of our model a determinant factor is the lattice topology. In the $\mathcal{C}$-classification we introduced, we showed that rules may behave completely differently when the size of the lattice is changed. They may switch from one category to another or even reveal new types of behavior.

The evolution from disordered states is a different fundamental approach. We worked with completely disordered states and observed the collective behavior of the $\mathcal{F}$-rule and particularly it's ability for self-organisation. The three types of behavior reported include: A coarsening evolution that leads to labyrinthine patterns. This state is strongly reminiscent of behavior observed with ferrofluids or magnetic bubbles [11] and also in classic probabilistic models such as the Voter's or the Ising model [7], [5]. The second type is this of the system's convergence to periodic cycles and is characterised by strong self-organisation. The system starts from an arbitrary initial state and follows a finite transient time (the duration of which we assume that depends on the size of the lattice) and settles down to periodicity. The governing dynamical feature of this case is the *ying-yang* type of oscillation which in the steady state satisfies (13). Moreover the system seems to have limited sensitity to initial conditions only during the transient mode. This phenomenon is known in the dynamical system theory as *transient chaos* [6]. The last case we met is this when one equal-state cost (a) gets in the middle of the cross-state costs (b, c with $b < c$). The result is a structurally unstable system which behaves aperiodically and is characterised by sensitivity to small perturbations. Rergarding the deterministic nature of our model we have every reason to believe that this is a chaotic behavior.

In the last section we attempted to extend the $\mathcal{F}$-rule to

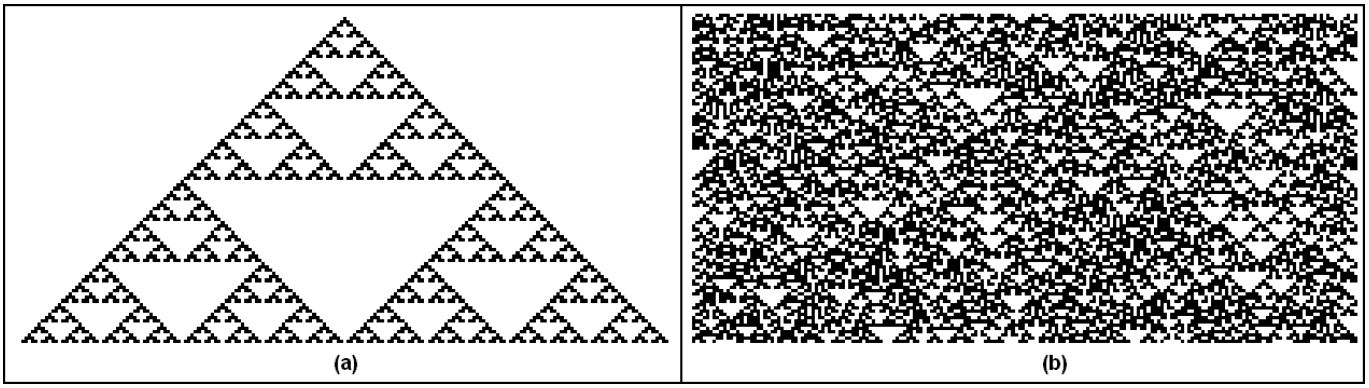

FIG. 14: The $\overline{\mathcal{F}}_{(0,b>2,c<b-1,1)}$-rule, as defined in text, in one dimension. The cost parameters are set for the rule to expand. However the resulting pattern is not uniform as in of the $\mathcal{F}$-rule. (a)Evolution from simple initial state. The resulting pattern is the self-similar *Sierpinski* fractal. (b) Evolution from disordered initial state. This is a typical chaotic pattern.

the field of Game Theory. Regarding a smart player that always plays as to maximize it's own profit we see how it's play effects the rest of the players. This quantifies the idea of how much robust is the decision function f_2 we examine. The simulation results show that depending on the selected cost parameteres the influence of the smart player can be neglibible, local, even global (Figs.12(a)-(c) respectively). This result is in direct conjunction with the rule's relevant instability.

C. Where do we go from here?

Up to this point, an extensive effort to explore a proposed mathematical model is made. In this section, we will make suggestions for further research. Furtheremore, we shall propose types of variations which we believe are of special interest. In the end, we will outline fields on which such model may be applicable. In this paper, our purpose is to study a new update rule in cellular automata and to shed light upon its perspectives. However, many more things are left to do. One line of research could be on the direction of phase transition diagrams which we outlined above. Moreover the inspection of the cost distribution and the overall behavior of the so-called $J(t)$ space is strongly recommended. The connecting factors between $G(t)$ and $J(t)$ pave the way for remarks upon the immitation and the cooperation features among the interacting cells. For example, one may define a cooperation criterion as the maximization of the global cost that can emerge under a certain amount of white cells, and then to search for the appopriate cost parameters to satisfy it.

D. Variations of the $\mathcal{F}$-rule

Perhaps, the most significant advantage of this model, is its structural flexibility. Conventional variations of cellular automata are the various definitions of neighborhoods $\mathcal{N}(\overrightarrow{x}, r)$ (*Moore* or *Von Neumann* scheme, among others [4]) or the state space topology (e.g. boundary conditions), the dimensionality of the rule ($\mathcal{L}^d$) or perhaps the number of elements in Σ. Apart from typical changes we can also vary our rule in terms of:

Cost function f_1. In this paper we assumed that at the end of every iteration, costs are reset to zero. Namely, we made use of instant costs upon the update decision of cells. Another version with significant physical meaning would be this of accumulative or discount costs per iteration. Each cell saves its cost values from previous states adding it on the future payoffs. For every iteration, a constant discount factor is multiplied with all past costs before the new cost is added. Preliminary simulations have revealed that the collective behavior of such automata is totally different.
Decision function f_2. We have assumed that the update rule defines the new state of site $\overrightarrow{x} : \sigma(\overrightarrow{x}; t+1)$ to equal to the state of its neighbor with the maximum cost. An already proposed variation is the $\mathcal{O}$-rule. Another important version though, would be that every $\overrightarrow{x} \; \epsilon \; \mathcal{L}$ do the following: It calculates the average costs among the same state neighbors. Then $\overrightarrow{x}$ decides to step to the state with the highest average cost. Of course, function f_2 could be configured to decide according to the minimum of costs. Such behaviors may also be observed in practice.

E. Applications

This automaton could reliably simulate procedures in many fields of life, some of which are reported below:
Social networks
If we consider $\mathcal{L}$ to be a compact society of citizens (cells), then white, $\sigma = 1$, state would adjust to a *good* man while the black, $\sigma = 0$, would adjust to the *bad* man. Our lat-

tice is, thus, a collection of concrete neighborhoods which interact, according to a cost function (eq. (6) or Fig. 2(a)), locally and eventually globally. So let's consider the neighborhood $\underline{\mathcal{N}}(\overrightarrow{x})$ of cells. Suppose that $\overrightarrow{x}$ is a good man with s also good neighbors and $(8-s)$ bad neighbors. Then, for every good $\overrightarrow{y}\ \epsilon\ \mathcal{N}(\overrightarrow{x})$, $\overrightarrow{x}$ gains a reward of d units while for every bad, our hero may get a penalty of c units. From this point of view, table cost is a locomotive regulator of interactions of "good" over "bad" and vice versa. Together with this regulator one can define static controllers as fixed regions of sites (perhaps on the boundary) whose value remain unchanged throughout simulation. Such areas would imitate the role of a church or a police station around a neighborhood. It is also worth mentioning the social meaning of the $\mathcal{O}$-rule by which a player learns to adaptate it's state judging from it's environment as to maximize it's personal profit. Both these rules are most usually observed social behaviors of every day life.

Economic Networks

Modelling market interaction. Economics is a subject of social networks, in which the procedure of learning or imitation and then reply among interacting individuals is fundamendal (a game theory approach can be found in [1]). In $\mathcal{F}$-realm, sites would be sellers and buyers. To make this more intriguing one could raise the number of possible states and then separates them in two categories: people who sell certain goods, and of people who buy them. Cost values would form the relative value between goods. Similar interpretation can be given for $\mathcal{O}$-model.

Other applications

Although strictly deterministic, the $\mathcal{F}$-rule produces patterns that bear great resemblance to stochastic models like the Voter's or the Ising model. This comes as no surprise, though, since both models preserve a probability distribution subject to local interaction among individuals. The Ising model, in particular, follows a Boltzman distribution with probabilities scaled according to an Energy function structurally similar to our cost function (6). It is worth mentioning that the three group of patterns generated from random seeds in sections **IV**A, **IV**B and **IV**C could be qualitatively connected to patterns of the 2D Ising model below, near and above the critical temperature, respectively [7]. It is important to clearify that this is the main difficulty in our model. The F-rule is a deterministic model with behavior that is in some cases similar to stochastic models. While, all such models are primarily defined by a global probability measure; what we deal with, is a local function that even easy to understand, it is most difficult to implement any analytical technique. That's how we end up simulating. Furthermore, deriving a probability measure out of direct simulations is not only a scientifically controversial method but also of forbidding computational complexity. Nevertheless, there is no doubt that our model can have potential applications in physical (statistical mechanics - lattice gas theory)[7, 15] or even biological (interaction between malignant and non-malignant cells) networks as well as in computer networks. However, further research on this model is required.

[1] Cartwright, E., 2007, Int. J. Game Theory **36**, 116.

[2] C.E Somarakis, G. P., and F. Udwadia, 2008, in *22nd European Conference on Modelling and Simulation*, pp. 164–170.

[3] Gardner, M., 1970, Scientific American , 120.

[4] Ilachinski, A., 2002, *Cellular Automata. A Discreet Universe* (World Scientific, NJ).

[5] J. D. Shore, M. H., and J. P. Sethna, 1992, Phys. Rev. B **46**(18), 11376.

[6] K. Alligood, T. S., and J. Yorke, 1996, *CHAOS. An introduction to dynamical systems* (Springer, NY).

[7] Kindermann, J., and J. Snell, 1980, *Markov Random Fields and Their Applications* (AMS, NY).

[8] Neumann, J. V., 1948, Celebral Mechanisms in Behavior - The Hixon Symposium , 1.

[9] Nowak, A., and R. May, 1992, Nature **359**, 826.

[10] Packard, N., 1985, Institute for Advanced Study (preprint).

[11] Rosensweig, R., 1979, Adv. Electronics Electron Phys. **48**, 103.

[12] Shereshevsky, M. A., 1992, J. Nonlinear Sci. **2**, 1.

[13] Tissuer, P., 2000, Nonlinearity **13**, 1547.

[14] Turing, A., 1952, Phil. Trans. R. Soc. London **237**(641), 37.

[15] U. Dieckmann, R. L., and J. Metz, 2000, *The Geometry of Ecological Interactions: Simplifying Spatial Complexity* (Cambridge University Press, UK).

[16] Wiederien, R., and F. Udwadia, 2004, Int. J. Bifurcation and Chaos **14**(8), 2555.

[17] Willson, S., 1978, Discrete Math. **23**, 279.

[18] Wolfram, S., 1984, Physica D **10**, 1.

[19] Wolfram, S., 2000, *Automata and Complexity. Collected Papers* (Addison-Wesley).

[20] Wolfram, S., and N. Packard, 1985, J. Stat. Phys. **38**, 901.

[21] The Moore scheme defines interaction of every cell with 8 neighbors, thus 8 possible directions of propagation.